Comunicações Geológicas, 2010, t. 97, pp. 63-70

Occurrence and Origin of Alluvial Xenotime from Central Eastern Portugal (Central Iberian Zone/Ossa-Morena Zone)

Ocorrência e Origem de Xenótimo Aluvionar do Centro-Leste de Portugal (Zona Centro-Ibérica/Zona de Ossa Morena)

D. Rosa*; R. Salgueiro**; C. Inverno*; D. de Oliveira* & F. Guimarães***

Keywords: Xenotime, alluvial, rare earths, CIZ/OMZ.

Abstract: Trace amounts of alluvial xenotime (YPO_4) were identified in black sands from pan concentrates collected during a rare earth reconnaissance survey, carried by the Instituto Geológico e Mineiro (IGM) in Central Eastern Portugal. The xenotime occurs as sub-rounded grains with an average size of ≈ 250 μm, and its identification was confirmed through XRD methods and EPMA analysis. It is believed that xenotime is more abundant than normally recognized and therefore frequently overlooked. The largest concentrations of this mineral occur in Nisa, S.to António das Areias and Marvão. The regional geology and the accompanying mineral suite suggest xenotime originates from the granitic massifs of Nisa and Penamacor as well as the Beira Baixa Arkoses and levels of Plio-Pleistocene gravels interspersed with sandy clay. Although its economic interest is presently limited, its demand may increase as a result of the potential use of yttrium in the manufacturing of superconductors that are stable at ambient temperature.

Palavras-chave: Xenótimo, aluvionar, terras raras, ZCI/ZOM.

Resumo: Foi identificado xenótimo (YPO_4) aluvionar em concentrados de bateia colhidos numa campanha de prospecção de terras raras desenvolvida pelo ex-IGM no centro-leste de Portugal. O xenótimo ocorre em grãos sub-rolados de dimensão média ≈ 250 μm e a sua identidade foi confirmada através de difracção de raios X e análises de microssonda electrónica. As concentrações mais significativas foram identificadas em Nisa, S.to António das Areias e Marvão. A geologia regional e o cortejo mineral das amostras sugerem que a proveniência do xenótimo possa estar nos maciços graníticos de Penamacor e Nisa e ainda as Arcoses da Beira Baixa e níveis de cascalheiras Plio-Plistocénicas com intercalações argilo-arenosas. Embora o seu interesse económico seja actualmente limitado, a procura deste mineral pode aumentar como resultado da potencial utilização de ítrio no fabrico de supercondutores estáveis à temperatura ambiente.

1. INTRODUCTION

Xenotime (YPO_4) is one of the few yttrium minerals known to science. This metal is used extensively in phosphors employed in television tubes and computer monitors and is also finding applications in special alloys, in laser systems and as a catalyst for ethylene polymerization (Hammond, 1997) and could become critical in the manufacturing of superconducting ceramics and rare earth magnets. Yttrium supply from monazite and xenotime placers is vast (worldwide reserves of 540.000 tons Y_2O_3). In 2009, production was dominated by China, which produced 8.800 tons of Y_2O_3, with remaining nations producing a total of less than 100 tons (USGS, 2010). However, yttrium demand is expected to rise if its application in superconductors stable at ambient temperature is confirmed, and these superconductors move out of the laboratory and into the marketplace. The second generation of superconductors, based on yttrium barium copper oxide, is called YBCO. According to 3M corporation, market research points to a potential market in the United States, Japan, and Europe for superconductor

* (LNEG; CREMINER-ISR, LA /FCUL) diogo.rosa@lneg.pt; carlos.inverno@lneg.pt; daniel.oliveira@lneg.pt
** (LNEG; CEGUL e CREMINER-ISR, LA / FCUL) rute.salgueiro@lneg.pt
*** (LNEG) fernanda.guimaraes@lneg.pt

products and services reaching 122 billion US dollars by the year 2020 (Morrison, 1999). This demand increase may spike yttrium oxide prices, presently around ≈ 50 USD/kg (USGS, 2010). Aware of the importance of rare earths (lanthanides, yttrium and scandium) for high-tech applications, namely for renewable energy technologies and hybrid vehicles, as well as of its importance in the global market for these products, China has started to restrain the exports of these elements and its ores, through the enforcement of export taxes and even prohibiting its exportation. These increasingly more restrictive export quotas by China support the emergence of alternative producers and therefore the identification of xenotime in Portugal is particularly relevant.

2. GEOLOGICAL SETTING

The identification of xenotime was the result of the study of 1962 pan samples (Table 1), collected in Central Eastern Portugal, within the framework of a reconnaissance survey targeted at the identification of rare earth mineral-bearing horizons, during 1995-2007 (Inverno *et al*., 2007).

TABLE 1

Studied 1/25,000 sheets and the relative abundance of xenotime.

1/25 000 sheets	Number of studied samples	% samples containing xenotime
258, Monsanto	129	20
269, S. Miguel d'Acha	232	5
270, Alcafozes	119	16
306-A, Rosmaninhal Leste	13	8
314,Vila Velha de Rodão	202	≥ 3
315, Montalvão (Nisa)	129	9
315-A, Montalvão-Este (Nisa)	54	13
315-B, Rosmaninhal Sul	26	23
324, Nisa	57	58
325, Póvoas e Meadas	148	28
325-A, Retorta	8	13
336, Sto António das Areias	81	78
348, Marvão	170	6
360, Alegrete	108	0
372, Assumar (Monforte)	134	1
383, Fronteira	352	1
TOTAL	**1962**	

The study area encompasses both the Central Iberian Zone (CIZ) and the Ossa-Morena Zone (OMZ) of the Variscan Orogen (Figure 1). The CIZ includes, from North to South, the Cambrian Schist-Greywacke Complex, intruded by granitic plutons at Idanha-a-Nova, Penamacor, Castelo Branco, Nisa and Portalegre, the Paleogene Beira Baixa Arkoses and related Mio-Pliocene sandstone and conglomerate formations and the Ordovician Quartzite ridges of Salvador – Penha Garcia – Monfortinho, Vila Velha de Ródão and Portalegre. The OMZ includes the Série Negra Formation in the Tomar-Cordoba Shear Zone and Ordovician peralkaline rocks and Cambrian meta-sedimentary rocks locally intruded by granitic plutons (Fronteira and Ervedal).

3. MATERIAL AND METHODS

The alluvial samples where panned and sieved to less than 3 mm at the sample locations. Density separation was done at the laboratory using bromoform (for d > 2.89). Subsequently, the heavy mineral fraction was split into a magnetic and a non-magnetic fraction using a hand magnet ($\geq 10\times10^{-6}$ C.G.S.M.E. units), and xenotime grains were handpicked from the magnetic fraction. Grains were analyzed with a Philips PW-1008 diffractometer, with Cu kα radiation, 40 kV voltage and 30 mA current. Electron-probe microanalyses (EPMA) were carried out using a fully automated JEOL JXA-8500F microprobe, equipped with one energy dispersive (EDS) and five wavelength dispersive (WDS) spectrometers, to analyze phosphorous, uranium, thorium, calcium, silicon, iron, lead and the rare earth elements. The operating conditions were accelerating voltage 20 kV, beam current 20 nA, beam diameter 2 μm and counting times for each element 20 s. For all the quantitative analysis the following standards were used: Almandine garnet (Si), synthetic YAG (Y), apatite (P, Ca), FeS_2 (Fe), UO_2 (U), ThO_2 (Th), Sc (Sc) and all the rare earth elements were analyzed using synthetic standards of LaP_5O_{14} (La), CeP_5O_{14} (Ce), PrP_5O_{14} (Pr), NdP_5O_{14} Nd), GdP_5O_{14} (Gd), SmP_5O_{14} (Sm), YbP_5O_{14} Yb), TmP_5O_{14} (Tm), ErP_5O_{14} (Er), HoP_5O_{14} (Ho), TbP_5O_{14} (Tb), DyP_5O_{14} (Dy), EuP_5O_{14} (Eu), LuP_5O_{14} (Lu).

4. CHARACTERIZATION OF XENOTIME GRAINS

Xenotime, which has a magnetic susceptibility which reaches above 18.9×10^{-6} C.G.S.M.E. units (Parfenoff *et al*., 1970), occurs within the magnetic fraction of the

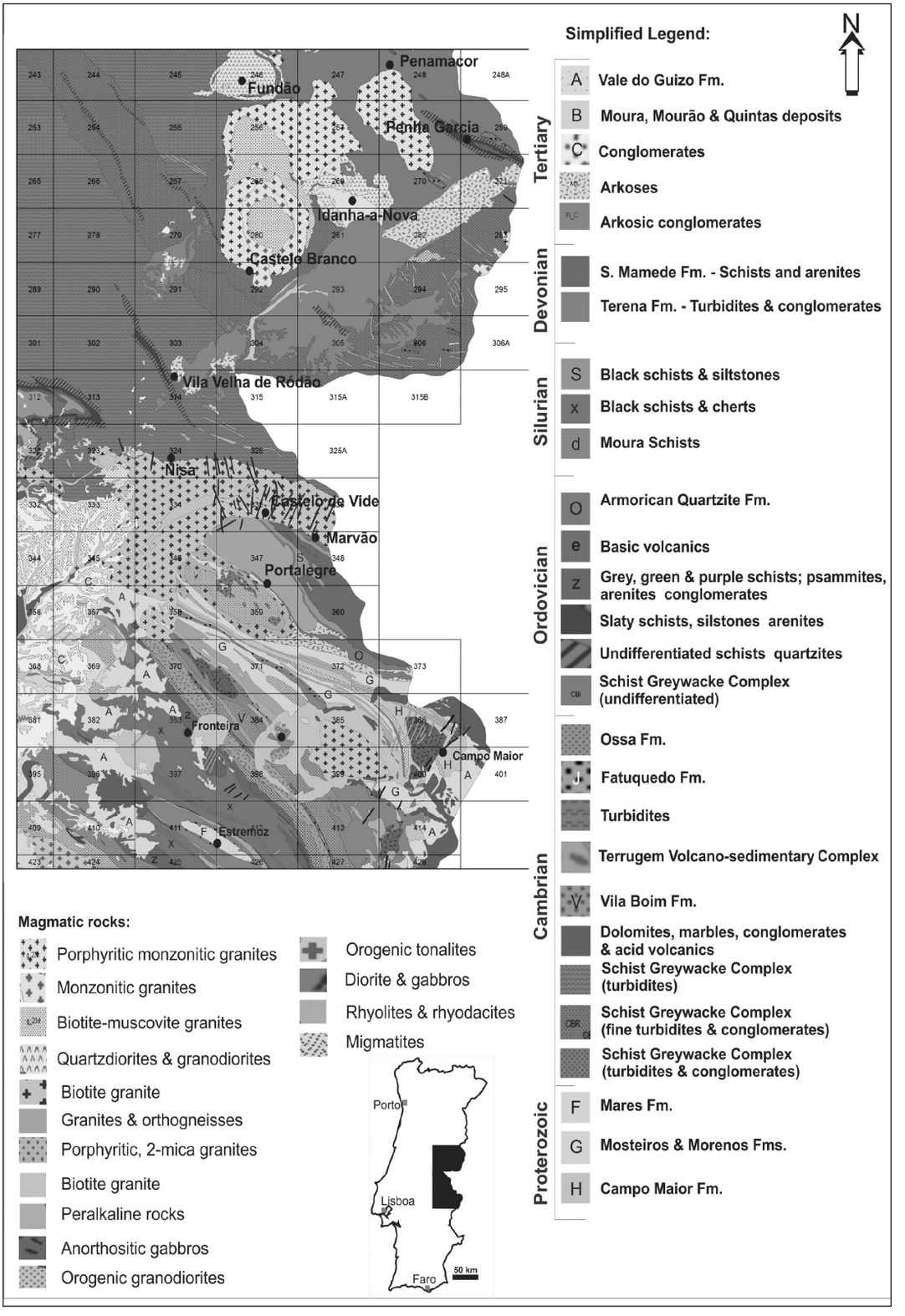

Fig. 1 – Geological setting of the Central Eastern Portugal (modified after OLIVEIRA *et al.*, 1992).

studied samples as rounded to sub-rounded grains, with pale green or yellowish brown colors and resinous luster. The grains range from 100 to 375 µm, averaging ≈ 250 µm (N = 39). In some instances, long or short prisms with bipyramidal terminations, of the tetragonal system can be identified (Figure 2), as described by Gaines *et al.* (1997). Electron back-scattered images reveal zoning and, occasionally, inclusions of monazite (Figure 3). In addition to these physical and morphological characteristics, the identity of this mineral was confirmed through X-ray diffraction. The X-ray diffraction profile (power method) of the analysed grains fits well with the xenotime 11-254 ASTM card, since it has characteristic X-ray lines (Figure 4) at 3.45 (100%), 2.56 (50%), 1.77 (50%), 4.55 (25%), 2.15 (25%), 2.44 (14%), 1.93 (10%), 1.82 (14%), 1.73 (18%), 1.54 (10%), 1.51 (4%), 1.43 (10%), 1.38 (8%), 1.28 (10%),1.24(10%) and 1.15 Å (8%) [JCPDS, 1980].

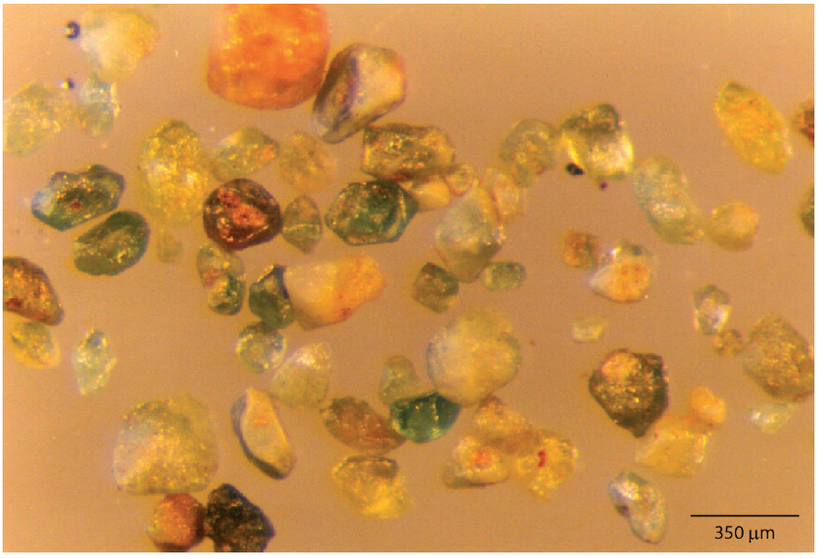

Fig. 2 – Xenotime grains (100%) from alluvial samples from the Vila Velha de Ródão area.

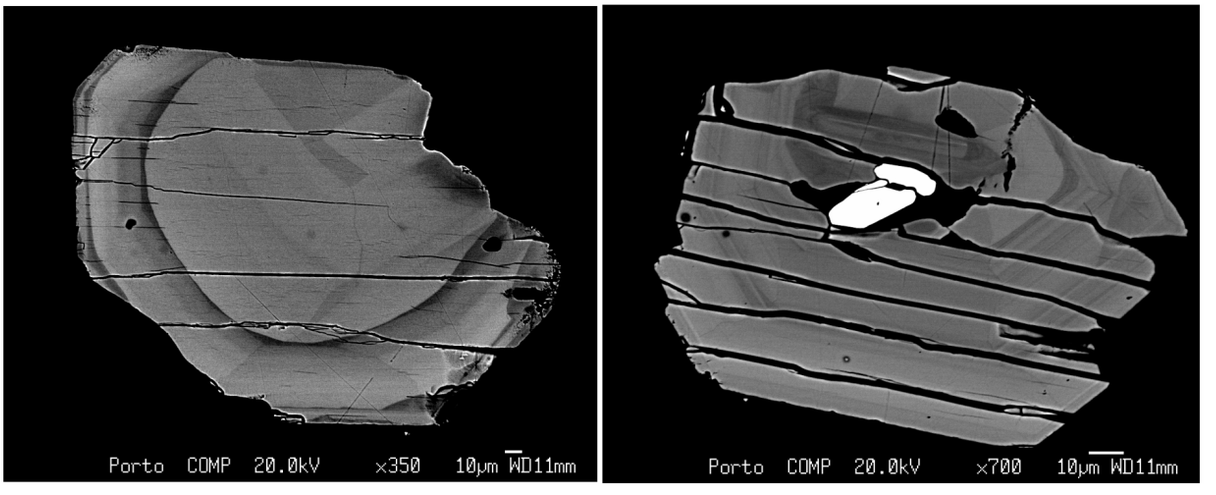

Fig. 3 – Backscattering electron images of xenotime grains (white inclusion on the image of the right is monazite).

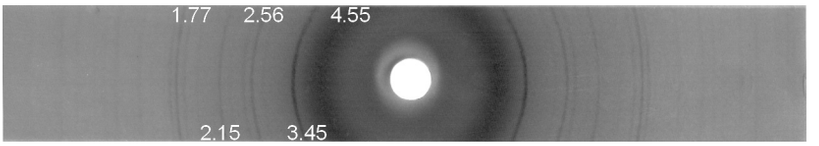

Fig. 4 – X-ray diffraction spectra of xenotime. The main five X-ray lines are indicated.

EPMA analyses of detrital xenotime grains from four different topographic sheets (Table 2) reveal relatively minor variations in chemical composition between the different sheets, though there is some variation within each sheet. The main substitutions of Y in xenotime are, in decreasing order, Dy, U, Gd, Er, Yb and Ho.

5. ORIGIN OF XENOTIME

Xenotime occurs in at least 240 out of the 1962 studied samples. Xenotime is particularly abundant in Nisa and S.^{to} António das Areias, where it is present in 58% and 78% of the studied samples, respectively (Table 1). While, in most samples xenotime represents ≤1 to 5% of the volume of magnetic fraction, in S.^{to} António das Areias and Marvão it can reach between 5 and 25% of this fraction (Table 3). Additionally, during this study it was evidenced that the areas richer in xenotime tend to supply samples with larger variety of associated minerals. In addition to xenotime, ilmenite and classical and nodular monazite are also frequent. Other minerals of interest include cassiterite, scheelite, wolframite and pyrite.

TABLE 2

EPMA analysis of xenotime grains.

	Topo Sheet 324 (N=9)			Topo Sheet 325 (N=3)			Topo Sheet 336 (N=7)			Topo Sheet 314 (N=15)		
	Min.	Max.	Average	Min.	Max.	Average	Min.	Max.	Average	Min.	Max.	Average
P_2O_5	34.52	37.34	35.74	34.93	37.08	36.13	35.84	37.42	36.58	35.93	37.88	36.70
Y_2O_3	37.69	41.68	39.66	38.24	41.76	40.46	38.14	40.59	39.27	37.72	41.16	39.35
UO_2	2.41	6.55	4.51	2.96	6.53	4.55	3.89	5.91	5.09	0.46	5.18	3.00
SiO_2	0.00	1.01	0.70	0.09	1.11	0.57	0.36	0.78	0.59	0.00	0.76	0.51
PbO	0.11	0.33	0.21	0.16	0.28	0.22	0.02	0.22	0.13	0.00	0.32	0.13
FeO	0.00	0.56	0.20	0.00	0.05	0.03	0.00	0.02	0.01	0.00	0.11	0.05
CaO	0.31	0.73	0.52	0.43	0.68	0.54	0.42	0.72	0.59	0.03	0.57	0.30
Sc_2O_3	0.03	0.08	0.04	0.06	0.07	0.07	0.01	0.08	0.05	0.00	0.07	0.04
ThO_2	0.13	0.43	0.29	0.11	0.45	0.23	0.19	0.45	0.33	0.00	1.35	0.38
La_2O_3	0.00	0.16	0.07	0.00	0.00	0.00	0.00	0.10	0.08	0.00	0.11	0.06
Ce_2O_3	0.12	0.35	0.19	0.01	0.18	0.11	0.00	0.21	0.13	0.00	0.24	0.12
Pr_2O_3	0.00	0.12	0.06	0.00	0.02	0.01	0.00	0.07	0.04	0.00	0.17	0.09
Nd_2O_3	0.30	0.64	0.46	0.20	0.53	0.36	0.34	0.58	0.46	0.29	0.61	0.44
Sm_2O_3	0.58	0.85	0.65	0.48	0.65	0.58	0.60	0.91	0.72	0.58	0.80	0.69
Eu_2O_3	0.00	0.04	0.02	0.00	0.00	0.00	0.00	0.02	0.01	0.00	0.03	0.03
Gd_2O_3	3.05	3.73	3.41	3.01	3.48	3.20	3.20	4.38	3.70	3.11	3.96	3.55
Tb_2O_3	0.00	0.44	0.49	0.49	0.56	0.53	0.51	0.75	0.63	0.40	0.61	0.51
Dy_2O_3	4.34	5.17	4.91	4.78	5.12	5.00	5.05	5.98	5.43	4.39	5.79	5.03
Ho_2O_3	0.93	1.23	1.09	1.00	1.19	1.12	1.02	1.32	1.18	0.93	1.34	1.17
Er_2O_3	3.24	3.64	3.44	3.24	3.42	3.36	2.77	3.41	3.10	3.28	4.35	3.73
Tm_2O_3	0.46	0.61	0.53	0.59	0.62	0.60	0.36	0.60	0.49	0.43	0.77	0.58
Yb_2O_3	2.95	3.59	3.27	2.98	3.31	3.20	2.51	3.39	2.78	3.06	5.84	3.67
Lu_2O_3	0.70	0.95	0.80	0.80	0.89	0.83	0.65	0.82	0.72	0.70	1.22	0.86

TABLE 3

Alluvial samples (pan concentrates): Percentage of xenotime (in magnetic fraction) and predominant minerals.

		Predominant minerals in the complete sample																			
	Xenótime (in the magnetic fraction)	Ilmenite	Garnet	Epidote s./	Leucoxene	Spinel	Iron oxides	Staurolite	Classical Monazite	Tourmaline	Andaluzite	Anatase	Zircon	Biotite	Rutile	Apatite	Pyrite	Wolframite	Scheelite	Others
Sheet 258	≤1%	x					x			x	x	x								Cassiterite, classical monazite, nodular monazite, apatite, zircon, rutile, chlorite, wolframite, gold and cinnabar.
Sheet 269	≤1%	x								x		x	x			x				Classical monazite, nodular monazite, iron oxides, andaluzite, topaz, cassiterite, wolframite, scheelite and gold.
Sheet 270	≤1%	x		x			x			x	x	x		x						Classical monazite, nodular monazite, rutile, anatase, brookite, garnet, apatite, zircon, topaz, muscovite, kyanite, sillimanite, cassiterite, scheelite and gold.
Sheet 306-A	≤1%	x			x		x													Tourmaline, zircon, epidote s.l., rutile, brookite, anatase, topaz, leucoxene, scheelite and gold.
Sheet 314	≤1%	x								x	x	x	x		x					Classical monazite, nodular monazite, topaz, staurolite, garnet, leucoxene, biotite, iron oxides, chalcopyrite, epidote, gold, cassiterite, cinnabar, brookite.
Sheet 315	≤1%	x					x			x	x		x				x			Classical monazite, nodular monazite, epidote s.l., staurolite, garnet, kyanite, sillimanite, apatite, rutile, anatase, brookite, topaz, leucoxene, biotite, apatite, gold scheelite and cinnabar.
Sheet 315-A	≤1%	x	x				x			x	x		x							Nodular monazite, classical monazite, pyrite, epidote s.l., staurolite, leucoxene, apatite, rutile, anatase, brookite, sillimanite, kyanite, topaz, gold, cassiterite, scheelite and cinnabar.
Sheet 315-B	≤1%	x					x	x	x				x						x	Pyrite, epidote s.l., tourmaline, garnet, leucoxene, spinel, apatite, rutile, anatase, andaluzite, sillimanite, kyanite, topaz and gold.
Sheet 324	≤1 a 5%	x					x			x	x		x							Classical monazite, nodular monazite, pyrite, epidote, staurolite, garnet, leucoxene, apatite, rutile, anatase, topaz, muscovite and scheelite.
Sheet 325	≤1 a 5%	x								x	x	x	x	x						Classical monazite, garnet, iron oxides, apatite, topaz, barite, gold, scheelite, cassiterite and cinnabar.
Sheet 325-A	1 a 5%	x								x	x			x						Classical monazite, epidote s.l., leucoxene, iron oxides, zircon, rutile, anatase, topaz, muscovite and scheelite.
Sheet 336	≤1 a 25%	x								x	x		x	x	x			x		Nodular monazite, classical monazite, pyrite, epidote s.l., staurolite, garnet, amphibole, leucoxene, iron oxides, spinel, pyrite, apatite, brookite, anatase, kyanite, sillimanite, topaz, barite, muscovite, gold, cassiterite, scheelite and cinnabar.
Sheet 348	≤1 a 25%	x					x			x	x	x	x	x						Classical monazite, nodular monazite, garnet, amphibole, leucoxene, apatite, rutile, scheelite and gold.
Sheet 372	≤1%	x	x	x		x	x		x											Pyrite, leucoxene, chlorite, zircon, rutile, anatase, andaluzite, kyanite, andaluzite, sillimanite, topaz and gold.
Sheet 383	≤1%	x	x	x	x	x	x	x												Classical monazite, tourmaline, amphibole, apatite, zircon, rutile, anatase, andaluzite, topaz, gold, cassiterite, scheelite and cinnabar.

Source rocks for xenotime are generally granites and pegmatites (GAINES *et al*., 1997; LARSEN, 1996), however xenotime can also be diagenetic and hydrothermal (*e.g.*, RASMUSSEN, 1996; KOSITCIN *et al*., 2003). Therefore, to constrain the source of the xenotime in the studied samples, the associated mineral suite was also characterized, as it reflects the local geology of the drainage basin and provides clues on the source of this mineral. In the areas of Penamacor-Monsanto (Sheets # 258, 269 and 270) and of Nisa-Castelo de Vide-Marvão (Sheets # 324, 325, 325-A, 336 and 348) xenotime is almost always associated with classical monazite, tourmaline, rutile, and zircon, reflecting a predominantly granitic source, resulting from the drainage of the Penamacor and Nisa granitic plutons, respectively. Complementarily, some other samples indicate a strong association of xenotime (together with classical monazite and, in places, apatite) with Beira Baixa Arkoses and levels of Plio-Pleistocene gravels interspersed with sandy clay (Sheets # 314, 315, 315-A and 315-B), and Paleogene-Miocene gravels, arenites, clays and marly limestones (Sheet # 383); in all these cases they may have included the results of the erosion of granite bodies (INVERNO *et al*., 2007). In contrast, the radioactive Ordovician quartzites of Salvador – Penha Garcia – Monfortinho (Sheets # 258 and 270) and Portalegre (Sheets # 360 and 372), which are rich in nodular monazite and REE (INVERNO *et al*., 1998), appear to be devoid of xenotime. The same seems to hold true for the Ordovician peralkaline rocks of the Tomar – Cordoba Shear Zone, since in only one alluvial sample (Sheet # 372) associated with them was xenotime found (< 1% of magnetic fraction) [Tables 1, 3].

The fact that diagenetic xenotime is described as occurring in small grains rarely exceeding 10 μm, which overgrow grains of detrital zircon (RASMUSSEN, 1996), also supports a granitic source, rather than a diagenetic source, for the coarser xenotime of this study. Additionally, the bipyramidal shape of the studied xenotime, evidenced in more preserved grains, indicates formation at a high temperature, which ultimately indicates granites and granitic pegmatites as the source rocks (SUBRAHMANYAM *et al*., 2004). Finally, trace element analysis concentrations of Gd, Dy and Eu (and its anomaly in a REE-pattern) confirm that this detrital xenotime has an igneous, rather than a diagenetic or hydrothermal, source (KOSITCIN *et al*., 2003).

6. CONCLUSIONS

The study of pan concentrates allowed the identification of significant amounts of xenotime in alluvial samples from Central Eastern Portugal. Dominantly, its association with classical monazite, tourmaline, rutile, and zircon, frequent bipyramidal shape, rather large size and its trace element concentrations is interpreted to indicate that this xenotime was mostly sourced from granitic rocks.

ACKNOWLEDGEMENTS

This work was done within the framework of a project financed by the European Union Cross-border INTERREG program.

The authors would like to thank Rosa Pateiro, Martim Chichorro and Helena Santana for their assistance in sample preparation and mineral identification under the binocular microscope.

The authors would also like to acknowledge Professors R.J. Santos Teixeira and A.M.R. Neiva for their constructive reviewing of this manuscript.

REFERENCES

GAINES, R.V., SKINNER, H.C.W., FORD E.E., MASON B. & ROSENZWEIG, A. (1997) – *Dana's New Mineralogy*, 8th Edition, Wiley Interscience, 1872 p.

HAMMOND, C.R. (1997) – *CRC Handbook of Chemistry and Physics*, 78th Edition. David R. Lide, Editor in Chief.

INVERNO, C.M.C., OLIVEIRA, D.P.S. & RODRIGUES, L., (colaboração de: VIEGAS, L., MATOS, J., MARTINS, L., SALGUEIRO, R., LENCASTRE, J., FARINHA, J., ROSA, D., CHICHORRO, M., SANTANA, H., OLIVEIRA, V., FERNANDES, J. & PATEIRO, R.) (2007) – Inventariação e prospecção de terras raras nas regiões fronteiriças da Beira Baixa e do Norte Alentejo: Alfragide, INETI, Internal Report, 2982 p.

INVERNO, C.M.C., OLIVEIRA, D.P.S., VIEGAS, L.F.S., LENCASTRE, J.P.B. & SALGUEIRO, R.M.M. (1998) – REE-enriched Ordovician quartzites in Vale de Cavalos, Portalegre, Portugal: *Proceedings Volume of GeoCongress'98*, Pretória, Jul.1998, Geological Society of South Africa, p. 153-157.

JCPDS (1980) – Mineral Powder Diffraction File Data Book. Joint Committee on Powder Diffraction Standards – International Centre for Diffraction Data, Pennsylvania, USA.

KOSITCIN, N., MCNAUGHTON, N.J., GRIFFIN, B.J., FLETCHER, I.R., GROVES, D.I. & RASMUSSEN, B. (2003) – Textural and geochemical discrimination between xenotime of different origin in the Archean Witwatersrand Basin, South Africa. *Geochimica et Cosmochimica Acta*, **67**, p. 701-731.

Larsen, A.O. (1996) – Rare earth minerals from the syenite pegmatites in the Oslo Region, Norway, *in* Jones, A. P., Wall, F., and Williams, C.T., eds, *Rare Earth Minerals – Chemistry, origin and ore deposits*. The Mineralogical Society Series, nr. 7, Chapman & Hall; London, U.K., p 151-166.

Morrison, G. (1999) – Superconductor power up, *Mechanical Engineering Magazine*, January 1999 issue.

Oliveira, J.T., Pereira, E., Ramalho, M., Antunes, M.T. & Monteiro, J.H. (compilers) (1992) – Carta Geológica de Portugal, 1: 500 000, Serviços Geológicos de Portugal, Lisboa.

Parfenoff, A., Pomerol, C., & Toureno, J. (1970) – *Les Minéraux en Grains – Méthodes d'étude et Détermination*. Paris, Masson et Cie, Éditeurs, 571 p.

Rasmussen, B. (1996) – Early-Diagenetic REE-phosphate minerals (florencite, gorceixite, crandalite, and xenotime) in marine sandstones: a major sink for oceanic phosphorus. *American Journal of Science*, **296**, p. 601-632.

Subrahmanyam A.V., Desapati, T., Anil Kumar V., Deshmukh, R.D. & Viswanathan G. (2004) – Occurrence of xenotime in the Narasapur beach placers, West Godavari District, *Current Science*, **87-10**, p. 1458-1461.

USGS (2010) – United States Geological Survey Mineral Commodity Summaries – Yttrium, January 2010.